Int. J. Heat Mass Transfer. Vol. 35, No. 7, pp. 1733–1741, 1992
Printed in Great Britain

0017-9310/92 $5.00+0.00

Laminar heat transfer for thermally developing flow in ducts

T. V. NGUYEN

CSIRO Division of Mineral and Process Engineering, P.O. Box 312, Clayton, Victoria 3168, Australia

(*Received* 31 *January* 1991 *and in final form* 4 *June* 1991)

Abstract—Laminar heat transfer in the entrance region of a circular duct and parallel plates is presented. The velocity profile is fully developed and the temperature is assumed to be uniform at upstream infinity. The finite difference equation for the energy equation, accounting for axial conduction, was solved by ADI and QUICK methods and the results extrapolated to zero mesh size with extended Richardson extrapolation. The local Nusselt number, incremental heat transfer number and thermal entrance length are presented for *Pe* between 1 and 1000; and for constant wall temperature and constant wall heat flux boundary conditions. Accurate engineering correlations for the Péclet number effect on these quantities were also obtained.

1. INTRODUCTION

THE ANALYSIS of heat transfer in the entrance region in ducts has been widely considered, and an extensive compilation of such solutions is provided by Shah and London [1]. In most of these studies, it was assumed that the velocity and temperature distributions at the entrance to the passage are uniform and the axial diffusion of both momentum and heat is negligible. In fact, if the pressure gradients and heat transfer rates were required near the entrance region, realistic boundary conditions of uniform flow far upstream must be used. The effect of the entrance region is to increase the pressure drop and the heat transfer rate. The additional pressure drop is caused by the momentum change and the accumulated increment in wall shear between developing flow and developed flow. This increment in the pressure drop over and above the fully developed value is designated as the incremental pressure drop number K and the increment in the heat transfer rate as the increment heat transfer number N. Accurate knowledge of K and N for ducts is of considerable practical as well as theoretical interest, especially the fully developed flow values, $K(\infty)$, $N_T(\infty)$ and $N_H(\infty)$. The effect of axial diffusion on fluid flow and heat transfer is negligible only at very high Reynolds and Péclet numbers, because of the rapid change in axial velocity and temperature gradients near the entrance. At low *Re* and *Pe*, K is a strong function of *Re* and N_T and N_H are strong functions of *Pe*.

This paper presents the results of a numerical study of the developed flow, laminar forced convection in the entrance region of a circular duct and parallel plates. The flow is fully developed and the temperature is assumed to be uniform at upstream infinity. Both constant axial wall temperature and constant and equal wall heat flux conditions along the ducts are studied. In most previous numerical solutions, the approximations of various parameters, such as the incremental pressure drop number $K(\infty)$ and the incremental heat transfer number $N(\infty)$, deteriorate at the end of the hydrodynamic or thermal entrance. In the present work, discretization error is reduced by extrapolating three mesh sizes to zero mesh size using the extended Richardson extrapolation. In addition, the QUICK scheme, which is well suited to the problem, is used with theoretically motivated stretched coordinates to improve accuracy and efficiency. The numerical results obtained are in excellent agreement with previous solutions, Nguyen and Maclaine-cross [2, 3] and Nguyen [4]. The local Nusselt number, incremental heat transfer number and thermal entrance length are presented for *Pe* ranging from 1 to 1000. Correlation equations are also given for all of the quantities considered.

2. THE EQUATIONS AND THEIR SOLUTION

This paper is concerned with the laminar heat transfer of a Newtonian constant property fluid at the entrance region of a circular duct and parallel plates of infinite extent. Viscous dissipation is neglected. The velocity profile is fully developed and the temperature profile is uniform at upstream infinity. The wall in the upstream region ($x < 0$) is assumed to be either insulated or at constant temperature. In the downstream region ($x \geqslant 0$) the wall is subject to the boundary condition of uniform wall temperature or uniform wall heat flux.

The dimensionless energy equation for steady laminar flow in a circular duct is given by

$$u\frac{\partial \theta}{\partial x} = \frac{1}{Pe}\left(\frac{\partial^2 \theta}{\partial r^2} + \frac{2}{(2r-1)}\frac{\partial \theta}{\partial r} + \frac{\partial^2 \theta}{\partial x^2}\right) \qquad (1)$$

NOMENCLATURE

D_h	hydraulic diameter
L^*_{th}	thermal entrance length
n	number of interior mesh points
N	incremental heat transfer number
$N(\infty)$	fully developed incremental heat transfer number
Nu	Nusselt number
Pe	Péclet number
Pr	Prandtl number
r	dimensionless radial coordinate
R	radius of circular duct
Re	Reynolds number, $D_h U_\infty/v$
T	temperature
T_w	wall temperature
T_∞	upstream temperature
u	dimensionless axial velocity
U_∞	upstream velocity
x	dimensionless axial coordinate
x^*	dimensionless axial coordinate for the thermal problem, $x/2Pe$
x_t	dimensionless transformed axial coordinate
y	dimensionless coordinate normal to the plates.

Greek symbols

α	thermal diffusivity
Δt	time step
ε	convergence factor
θ	dimensionless temperature
v	kinetic viscosity.

Subscripts

bc	thermal boundary condition
H	constant heat flux boundary condition
m	mean
t	transformed
T	constant temperature boundary condition
x	local
∞	free stream value.

in which $\theta = (T-T_\infty)/(T_w-T_\infty)$, $Pe = Re\,Pr$, $Re = U_\infty D_h/v$ and $Pr = v/\alpha$. Here R, v and α denote respectively the radius of the circular duct, the kinetic viscosity and the thermal diffusivity.

For parallel plates, the energy equation is as follows:

$$u\frac{\partial\theta}{\partial x} = \frac{1}{Pe}\left(\frac{\partial^2\theta}{\partial x^2}+\frac{\partial^2\theta}{\partial y^2}\right). \quad (2)$$

The streamwise coordinate and partial differential equations (1) and (2) were transformed both upstream and downstream of the entrance using a function related to the downstream decay [5]. The transformed coordinate x_t is dimensionless and $-1 \leqslant x_t \leqslant 1$. It may be calculated from the dimensionless coordinate x in equations (1) and (2) using

$$x_t = \frac{(1-\exp(-|x|/(0.089275Pe)))x}{|x|}. \quad (3)$$

The transformed coordinates give a more equal change in dependent variables over each grid element and points at downstream infinity. The number of grid elements required for a given discretization error is greatly reduced at the expense of slightly more computation per grid element.

Finite difference equations were derived from the transformed non-linear partial differential equations. Quadratic upstream interpolation for convective kinematics (QUICK) [6] was used for the convective terms to give stability with a discretization error of the order of the square of the mesh size. The alternating direction implicit (ADI) iterative method was used to solve the non-linear finite difference equations. Convergence was measured by calculating

$$\varepsilon_\theta = \frac{1}{n\theta_{max}}\sum\frac{\theta^{n+1}-\theta^n}{\Delta t} \quad (4)$$

where n is the number of interior mesh points, θ_{max} is the maximum magnitude of θ and Δt is the time step. Iteration was repeated until ε_θ were all less than 10^{-9} so that the error in solving the finite difference equations was negligible and independent of grid size.

The dimensionless groups used in the present work are defined as follows:

the local Nusselt number

$$Nu_x = \left(\frac{\partial\theta}{\partial r}\right)_{r=0}\bigg/(\theta_w-\theta_m) \quad \text{for circular duct} \quad (5)$$

$$Nu_x = 2\left(\frac{\partial\theta}{\partial y}\right)_{y=0}\bigg/(\theta_w-\theta_m) \quad \text{for parallel plates} \quad (6)$$

where θ_m is the fluid bulk mean temperature

the mean Nusselt number

$$Nu_m = \frac{1}{x}\int_0^x Nu_x\,dx \quad (7)$$

the incremental heat transfer number

$$N_{bc} = (Nu_{m,bc}-Nu_{bc})x^*. \quad (8)$$

The suffix bc represents the associated thermal boundary conditions (T or H) and Nu_{bc} is the Nusselt number for fully developed flow. The mean Nusselt number Nu_m is obtained by the integral in equation (7) for values of x up to $x = \infty$. The fully developed incremental heat transfer number $N(\infty)$ is then taken as the asymptotic value which N_{bc}, calculated by equation (8), converges to four significant figures.

Discretization error is the difference between the exact solution of the finite difference equations and the exact solution of the consistent partial differential equations. For the finite difference equations used here this is of the order of the grid size squared. It may be reduced to fourth order by extrapolation to zero grid size of the finite difference equation solutions for three different grid sizes. Each grid is solved with the same parameters and boundary conditions. The three grids chosen were 11×81, 21×161 and 41×321 mesh points in the r or y and x direction respectively making each grid size half its predecessor. The following extrapolation formula was calculated from the general expression in Maclaine-cross [5]:

$$A = A3 - \frac{(A3-A1)-12(A3-A2)}{21} \tag{9}$$

where $A3$ is the value at the smallest grid size, etc. It should be noted that the above formula is valid only for grids formed by successive mesh doubling, for numerical methods which are uniformly second-order accurate, and for very tight iterative convergence. Other details of the solution method are discussed elsewhere [7].

3. CIRCULAR DUCT

Equations (1) and (2) have been solved for the following Pe values: 1, 2, 5, 10, 20, 50, 100, 200 and 1000. It should be emphasized that Re is based on the hydraulic diameter $D_h = 2R$.

3.1. *Constant wall temperature results*

For the case of negligible axial heat conduction, the fully developed Nusselt number for a circular duct with the constant wall temperature boundary condition is 3.6568. However, when the effect of axial heat conduction in the fluid is included, the fully developed Nusselt number Nu_T is a strong function of the Péclet number for low Péclet number flows as shown in Table 1, where the results from the present numerical work and Shah and London [1] are listed. The present work is seen to be in excellent agreement with the values given in Shah and London.

Table 1. Circular duct: fully developed Nu_T as a function of Pe for the initial and boundary condition of Fig. 1(a)

Pe	Present solution	Ref. [1]
1	4.0280	4.030
2	3.9226	3.925
5	3.7673	3.769
10	3.6973	3.697
20	3.6675	3.670
50	3.6586	3.660
100	3.6572	—
200	3.6569	—
1000	3.6568	3.6568

For the case of a circular duct with boundary conditions of Fig. 1(a), the extrapolated values of the fully developed incremental heat transfer number $N_T(\infty)$ and the dimensionless thermal entrance length $L^*_{th,T}$, defined by $Nu_{x,T}(L_{th,T}) = 1.05 Nu_T$, are given in Table 2.

The following correlations can be used to approximate $N_T(\infty)$ in Table 2 with the error ranging from 0.35% at $Pe = 100$ to 4.89% at $Pe = 5$:

$$N_T(\infty) = -0.1577+2.5166/Pe, \quad \text{for} \quad 1 \leqslant Pe \leqslant 5 \tag{10}$$

$$N_T(\infty) = 0.00186+1.8024/Pe, \quad \text{for} \quad 5 \leqslant Pe \leqslant 20 \tag{11}$$

$$N_T(\infty) = 0.03596+1.1523/Pe, \quad \text{for} \quad 20 \leqslant Pe \leqslant 100 \tag{12}$$

$$N_T(\infty) = 0.04539+0.3515/Pe, \quad \text{for} \quad 100 \leqslant Pe \leqslant 1000. \tag{13}$$

Equations (14)–(16) correlate the values of $L^*_{th,T}$ given in Table 2 with the deviation ranging from 0.2% at $Pe = 1$ to 4.1% at $Pe = 10$

$$L^*_{th,T} = -0.003079+0.4663/Pe, \quad \text{for} \quad 1 \leqslant Pe \leqslant 5 \tag{14}$$

$$L^*_{th,T} = 0.02020+0.3550/Pe, \quad \text{for} \quad 5 \leqslant Pe \leqslant 20 \tag{15}$$

$$L^*_{th,T} = 0.03258+0.1295/Pe, \quad \text{for} \quad 20 \leqslant Pe \leqslant 1000. \tag{16}$$

Table 3 tabulates the extrapolated values of $N_T(\infty)$ and $L^*_{th,T}$ for all Pe for a circular duct with an adiabatic wall upstream from the entrance (Fig. 1(b)). The following equations are proposed for $N_T(\infty)$ in Table 3 to cover the complete Pe range with the error ranging from 0.08% at $Pe = 100$ to 3.8% at $Pe = 5$:

$$N_T(\infty) = -0.03044+0.9061/Pe, \quad \text{for} \quad 1 \leqslant Pe \leqslant 5 \tag{17}$$

$$N_T(\infty) = 0.02667+0.6466/Pe, \quad \text{for} \quad 5 \leqslant Pe \leqslant 20 \tag{18}$$

$$N_T(\infty) = 0.04301+0.3472/Pe, \quad \text{for} \quad 20 \leqslant Pe \leqslant 100 \tag{19}$$

$$N_T(\infty) = 0.04539+0.07664/Pe, \quad \text{for} \quad 100 \leqslant Pe \leqslant 1000. \tag{20}$$

For the thermal entrance length in Table 3, the following correlations are given to approximate $L^*_{th,T}$ to within 4.3%:

$$L^*_{th,T} = 0.000501+0.3829/Pe, \quad \text{for} \quad 1 \leqslant Pe \leqslant 5 \tag{21}$$

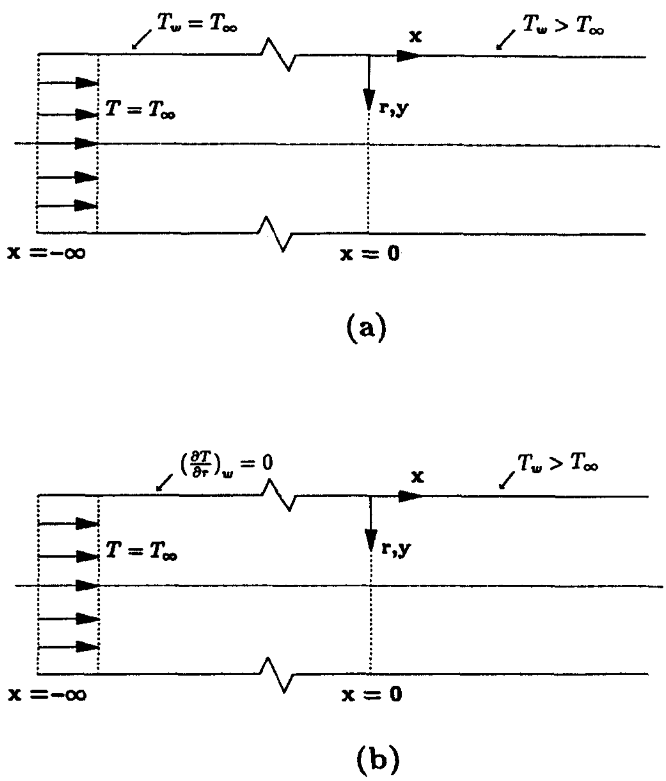

FIG. 1. Initial and boundary conditions for the case of constant wall temperature.

$$L^*_{\mathrm{th,T}} = 0.02154+0.2821/Pe, \quad \text{for} \quad 5 \leqslant Pe \leqslant 20 \tag{22}$$

$$L^*_{\mathrm{th,T}} = 0.03282+0.07852/Pe, \quad \text{for} \quad 20 \leqslant Pe \leqslant 1000. \tag{23}$$

The values of $N_T(\infty)$ of 0.04596 and 0.04644 at $Pe = 1000$ in the present study (uniform temperature profile at upstream infinity) are about 8% and 6.9% lower than the value (0.04990) given by the Graetz solution (uniform temperature profile at entrance). However, the thermal entrance lengths of 0.03330 and 0.03333 are very close to that from the Graetz solution (0.03346).

3.2. *Constant wall heat flux results*

In the case of constant wall heat flux, the axial heat conduction within the fluid is constant and therefore does not affect the Nusselt number. The fully developed, asymptotic local Nusselt number in this case is 4.3636 and is independent of the Péclet number. Table 4 presents the extrapolated local Nusselt number as a function of x^* for the whole range of Pe considered here. As seen from Fig. 2, which presents graphically the results from Table 4, the $Nu_{x,\mathrm{H}}$ vs x^* curves have an inflection point at $x^* \simeq 0.0077$, i.e. $Nu_{x,\mathrm{H}}$ increases with decreasing Pe. This phenomenon has also been found by previous workers, e.g. Hennecke [8] and Hsu [9], for the case of uniform entrance

Table 2. Circular duct: $N_T(\infty)$ and $L^*_{\mathrm{th,T}}$ for the initial and boundary conditions of Fig. 1(a)

Pe	$N_T(\infty)$	$L^*_{\mathrm{th,T}}$
1	2.3696	0.4643
2	1.0722	0.2273
5	0.3634	0.09193
10	0.1789	0.05352
20	0.09411	0.03940
50	0.05688	0.03437
100	0.04908	0.03357
200	0.04676	0.03337
1000	0.04596	0.03330

Table 3. Circular duct: $N_T(\infty)$ and $L^*_{\mathrm{th,T}}$ for the initial and boundary conditions of Fig. 1(b)

Pe	$N_T(\infty)$	$L^*_{\mathrm{th,T}}$
1	0.8793	0.3843
2	0.4130	0.1894
5	0.1568	0.07865
10	0.08895	0.04768
20	0.06058	0.03702
50	0.04910	0.03375
100	0.04712	0.03340
200	0.04661	0.03335
1000	0.04644	0.03333

Table 4. Circular duct: $Nu_{x,H}$ as a function of x^* and Pe

x^*	$Nu_{x,H}$							
	$Pe = 1$	2	5	10	20	50	100	1000
0	7.1240	7.4735	8.5176	10.2507	13.2274	19.4221	25.3311	36.8639
0.0005	7.0873	7.4014	8.2961	9.6586	11.5982	14.0941	15.0888	15.4544
0.001013	7.0506	7.3311	8.0959	9.1837	10.5427	11.8942	12.2544	12.3372
0.001540	7.0139	7.2626	7.9132	8.7896	9.7797	10.5990	10.7619	10.7882
0.002081	6.9773	7.1957	7.7454	8.4540	9.1900	9.7135	9.7938	9.8020
0.002637	6.9406	7.1302	7.5900	8.1623	8.7136	9.0559	9.0958	9.0967
0.003799	6.8672	7.0034	7.3100	7.6742	7.9786	8.1222	8.1279	8.1237
0.005033	6.7934	6.8811	7.0622	7.2759	7.4275	7.4740	7.4675	7.4620
0.006350	6.7191	6.7626	6.8391	6.9400	6.9921	6.9868	6.9756	6.9700
0.007762	6.6441	6.6472	6.6354	6.6502	6.6353	6.6014	6.5884	6.5829
0.010087	6.5296	6.4784	6.3579	6.2788	6.2012	6.1463	6.1330	6.1279
0.015768	6.2890	6.1476	5.8728	5.6881	5.5585	5.4947	5.4830	5.4789
0.020731	6.1138	5.9233	5.5814	5.3670	5.2313	5.1713	5.1611	5.1576
0.025493	5.9691	5.7467	5.3709	5.1506	5.0196	4.9649	4.9559	4.9528
0.034419	5.7444	5.4858	5.0884	4.8826	4.7685	4.7238	4.7167	4.7142
0.051151	5.4369	5.1507	4.7709	4.6207	4.5403	4.5133	4.5078	4.5047

temperature profile at upstream infinity. While the value of $Nu_{x,H}$ is infinite at the entrance for the case of uniform temperature profile at the entrance, the local Nusselt number has a finite value at $x^* = 0$ in the present study. The local Nusselt number at $Pe = 1000$ is slightly lower than the values for $Pe = \infty$ given in Shah and London, and generally lower than values from Hennecke given in Shah and London for $Pe = 1, 2, 5, 10, 20, 50$ and ∞.

For the case of constant wall heat flux, the extrapolated fully developed incremental heat transfer number and thermal entrance length for the boundary conditions of Figs. 3(a) and (b) are presented in Tables 5 and 6, respectively.

For $1 \leqslant Pe \leqslant 1000$, the following correlations are provided to approximate the values of $N_T(\infty)$ in Table 5 with the error ranging from 0.32% at $Pe = 200$ to 5.5% at $Pe = 2$:

$$N_T(\infty) = -0.07918 + 2.0509/Pe, \quad \text{for} \quad 1 \leqslant Pe \leqslant 10 \tag{24}$$

$$N_T(\infty) = 0.05278 + 0.7546/Pe, \quad \text{for} \quad 10 \leqslant Pe \leqslant 50 \tag{25}$$

$$N_T(\infty) = 0.06660 + 0.1660/Pe, \quad \text{for} \quad 50 \leqslant Pe \leqslant 1000. \tag{26}$$

The dimensionless thermal entrance length $L^*_{th,H}$ presented in Table 5 can be calculated from the following equation with the deviation ranging from 0.22% at $Pe = 1$ to 2.4% at $Pe = 10$:

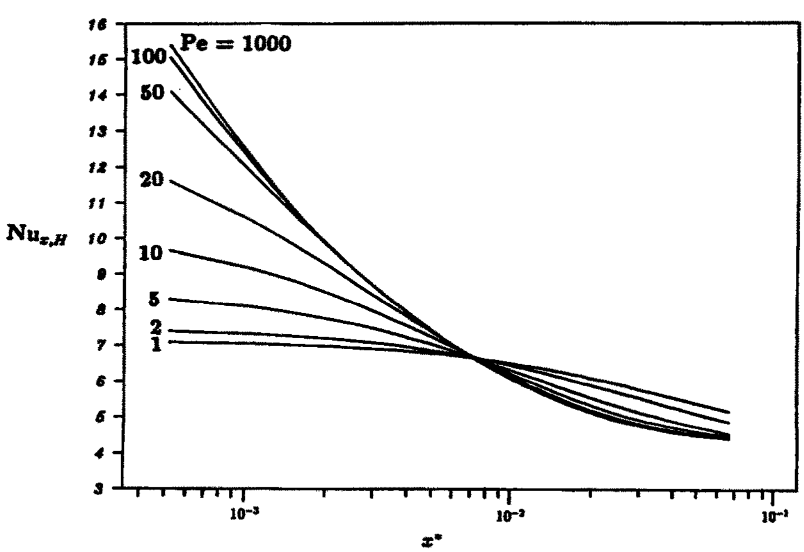

FIG. 2. Circular duct: $Nu_{x,H}$ as a function of x^* and Pe for the initial and boundary conditions of Fig. 3(b).

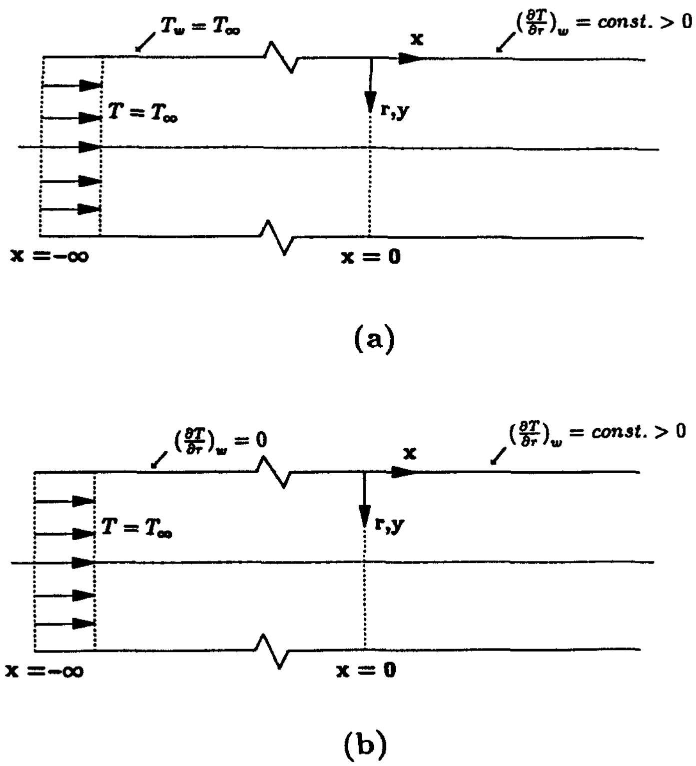

FIG. 3. Initial and boundary conditions for the case of constant wall heat flux.

$$L^*_{th,H} = -0.000518+0.4686/Pe, \quad \text{for} \quad 1 \leqslant Pe \leqslant 5 \tag{27}$$

$$L^*_{th,H} = 0.03263+0.3090/Pe, \quad \text{for} \quad 5 \leqslant Pe \leqslant 20 \tag{28}$$

$$L^*_{th,H} = 0.04217+0.1309/Pe, \quad \text{for} \quad 20 \leqslant Pe \leqslant 1000. \tag{29}$$

$N_H(\infty)$ and $L^*_{th,H}$ in Table 6 can be approximated by the following correlations with the error ranging from 0.13% at $Pe = 200$ to 3.4% at $Pe = 2$ for $N_H(\infty)$:

$$N_H(\infty) = 0.0426+0.1855/Pe, \quad \text{for} \quad 1 \leqslant Pe \leqslant 5 \tag{30}$$

$$N_H(\infty) = 0.05675+0.1264/Pe, \quad \text{for} \quad 5 \leqslant Pe \leqslant 20 \tag{31}$$

$$N_H(\infty) = 0.06401, \quad \text{for} \quad 20 \leqslant Pe \leqslant 50 \tag{32}$$

$$N_H(\infty) = 0.06775-0.1693/Pe, \quad \text{for} \quad 50 \leqslant Pe \leqslant 1000 \tag{33}$$

and from 0.22% at $Pe = 1$ to 1.39% at $Pe = 10$ for $L^*_{th,H}$

$$L^*_{th,H} = 0.03120+0.2131/Pe, \quad \text{for} \quad 1 \leqslant Pe \leqslant 5 \tag{34}$$

$$L^*_{th,H} = 0.03644+0.1901/Pe, \quad \text{for} \quad 5 \leqslant Pe \leqslant 20 \tag{35}$$

Table 5. Circular duct: $N_H(\infty)$ and $L^*_{th,H}$ for the initial and boundary conditions of Fig. 3(a)

Pe	$N_H(\infty)$	$L^*_{th,H}$
1	1.9641	0.4691
2	0.9577	0.2311
5	0.3138	0.09493
10	0.1293	0.06204
20	0.08767	0.04907
50	0.06964	0.04397
100	0.06911	0.04324
200	0.06726	0.04297
1000	0.06656	0.04287

Table 6. Circular duct: $N_H(\infty)$ and $L^*_{th,H}$ for the initial and boundary conditions of Fig. 3(b)

Pe	$N_H(\infty)$	$L^*_{th,H}$
1	0.2298	0.2448
2	0.1309	0.1363
5	0.08249	0.07471
10	0.06796	0.05469
20	0.06401	0.04645
50	0.06402	0.04340
100	0.06674	0.04302
200	0.06699	0.04294
1000	0.06715	0.04290

$$L^*_{th,H} = 0.04245 + 0.07531/Pe, \quad \text{for} \quad 20 \leqslant Pe \leqslant 1000. \quad (36)$$

The values of $N_H(\infty)$ of 0.06656 and 0.06715 at $Pe = 1000$ given in Tables 5 and 6 are about 7.8% and 7%, respectively, lower than the value of 0.0722 given by the Graetz solution. However, the thermal entrance lengths of 0.04287 and 0.04290 are very close to that from the Gratez solution (0.04305).

4. PARALLEL PLATES

4.1. *Constant wall temperature results*

As in the case of a circular duct, the fully developed Nusselt number for parallel plates with the constant wall temperature boundary condition is a strong function of Pe for low Pe values. This is shown in Table 7 and, for comparison purposes, an additional solution at $Pe = 1.4354$ was obtained and the predicted Nusselt number (7.9635) is in excellent agreement with 7.964 given in Shah and London.

For parallel plates, the extrapolated $N_T(\infty)$ and $L^*_{th,T}$ are given in Tables 8 and 9 for the case of the constant wall temperature boundary condition.

For $1 \leqslant Pe \leqslant 1000$, the following correlations can be used to approximate the data in Table 8 with the error ranging from 0.03% at $Pe = 1$ to 3.0% at $Pe = 50$ for $N_T(\infty)$:

$$N_T(\infty) = -0.0940 + 2.4333/Pe, \quad \text{for} \quad 1 \leqslant Pe \leqslant 10 \quad (37)$$

Table 7. Parallel plates: fully developed Nu_T as a function of Pe for the initial and boundary conditions of Fig. 1(a)

Pe	Present solution
1	8.0058
1.4354	7.9635
2	7.9164
5	7.7468
10	7.6306
20	7.5692
50	7.5456
100	7.5407
1000	7.5407

Table 8. Parallel plates: $N_T(\infty)$ and $L^*_{th,T}$ for the initial and boundary conditions of Fig. 1(a)

Pe	$N_T(\infty)$	$L^*_{th,T}$
1	2.3388	0.2334
2	1.1251	0.1125
5	0.3884	0.04354
10	0.1518	0.02198
20	0.07561	0.01291
50	0.03385	0.00891
100	0.02723	0.008214
200	0.02316	0.007946
1000	0.02172	0.007939

Table 9. Parallel plates: $N_T(\infty)$ and $L^*_{th,T}$ for the initial and boundary conditions of Fig. 1(b)

Pe	$N_T(\infty)$	$L^*_{th,T}$
1	0.7711	0.1844
2	0.3768	0.09031
5	0.1424	0.03550
10	0.06687	0.01855
20	0.03903	0.01141
50	0.02491	0.00845
100	0.02311	0.008046
200	0.02220	0.007957
1000	0.02189	0.007944

$$N_T(\infty) = 0.003253 + 1.4794/Pe, \quad \text{for} \quad 10 \leqslant Pe \leqslant 50 \quad (38)$$

$$N_T(\infty) = 0.02056 + 0.6593/Pe, \quad \text{for} \quad 50 \leqslant Pe \leqslant 1000 \quad (39)$$

and from 0.23% at $Pe = 1$ to 3.8% at $Pe = 50$ for $L^*_{th,T}$

$$L^*_{th,T} = -0.004930 + 0.2378/Pe, \quad \text{for} \quad 1 \leqslant Pe \leqslant 5 \quad (40)$$

$$L^*_{th,T} = 0.00213 + 0.2058/Pe, \quad \text{for} \quad 5 \leqslant Pe \leqslant 20 \quad (41)$$

$$L^*_{th,T} = 0.006783 + 0.1211/Pe, \quad \text{for} \quad 20 \leqslant Pe \leqslant 100 \quad (42)$$

$$L^*_{th,T} = 0.007865 + 0.0315/Pe, \quad \text{for} \quad 100 \leqslant Pe \leqslant 1000. \quad (43)$$

The data in Table 9 can be calculated from the following equations with a maximum error of 2.7% for $N_T(\infty)$ and 3.2% for $L^*_{th,T}$:

$$N_T(\infty) = -0.0133 + 0.7836/Pe, \quad \text{for} \quad 1 \leqslant Pe \leqslant 10 \quad (44)$$

$$N_T(\infty) = 0.01369 + 0.5278/Pe, \quad \text{for} \quad 10 \leqslant Pe \leqslant 50 \quad (45)$$

$$N_T(\infty) = 0.02155 + 0.1644/Pe, \quad \text{for} \quad 50 \leqslant Pe \leqslant 1000 \quad (46)$$

$$L^*_{th,T} = -0.002186 + 0.1863/Pe, \quad \text{for} \quad 1 \leqslant Pe \leqslant 5 \quad (47)$$

$$L^*_{th,T} = 0.002935 + 0.1619/Pe, \quad \text{for} \quad 5 \leqslant Pe \leqslant 20 \quad (48)$$

$$L^*_{th,T} = 0.00697 + 0.08746/Pe, \quad \text{for} \quad 20 \leqslant Pe \leqslant 100 \quad (49)$$

$$L^*_{th,T} = 0.01143 + 0.0450/Pe, \quad \text{for} \quad 100 \leqslant Pe \leqslant 1000. \quad (50)$$

$N_T(\infty)$ at $Pe = 1000$ from Tables 8 and 9 are about 7.5% and 6.8%, respectively, lower than the value of 0.02348 given in Shah and London [1] for the case of a uniform temperature profile at the entrance, and the thermal entrance lengths of 0.007939 and 0.007944 are very close to Shah and London's value of 0.007973.

4.2. *Constant wall heat flux results*

The fully developed Nusselt number for parallel plates with the constant wall heat flux boundary condition is 8.2353 and is independent of the Péclet number. The $Nu_{x,H}$ vs x^* curves for this thermal entrance problem with finite fluid axial heat conduction have an inflection point, similar to the circular duct case (see Shah and London [1] and Hsu [9]). Tables 10 and 11 present the extrapolated fully developed incremental heat transfer number $N_H(\infty)$ and the dimensionless thermal entrance length $L^*_{th,H}$ obtained in the present work.

For $1 \leqslant Pe \leqslant 1000$, the following correlations are provided to approximate the values of $N_H(\infty)$ and $L^*_{th,H}$ in Table 10 with the error ranging from 0.1% at $Pe = 50$ to 5.3% at $Pe = 50$ for $N_H(\infty)$ and with a maximum deviation of 4.5% for $L^*_{th,H}$:

$$N_H(\infty) = -0.1539+2.8563/Pe, \quad \text{for} \quad 1 \leqslant Pe \leqslant 10 \tag{51}$$

$$N_H(\infty) = 0.01633+1.1664/Pe, \quad \text{for} \quad 10 \leqslant Pe \leqslant 50 \tag{52}$$

$$N_H(\infty) = 0.03335+0.4284/Pe, \quad \text{for} \quad 50 \leqslant Pe \leqslant 1000 \tag{53}$$

$$L^*_{th,H} = -0.01283+0.3024/Pe, \quad \text{for} \quad 1 \leqslant Pe \leqslant 5 \tag{54}$$

$$L^*_{th,H} = 0.00603+0.2177/Pe, \quad \text{for} \quad 5 \leqslant Pe \leqslant 20 \tag{55}$$

$$L^*_{th,H} = 0.01091+0.1239/Pe, \quad \text{for} \quad 20 \leqslant Pe \leqslant 1000. \tag{56}$$

The data in Table 11 can be calculated by the following equations with the error ranging from 0.05% at $Pe = 200$ to 4.6% at $Pe = 50$ for $N_H(\infty)$ and from 0.11% at $Pe = 5$ to 3.7% at $Pe = 50$ for $L^*_{th,H}$:

$$N_H(\infty) = 0.01604+0.2681/Pe, \quad \text{for} \quad 1 \leqslant Pe \leqslant 5 \tag{57}$$

$$N_H(\infty) = 0.02706+0.2261/Pe, \quad \text{for} \quad 5 \leqslant Pe \leqslant 50 \tag{58}$$

$$N_H(\infty) = 0.03406-0.4500/Pe, \quad \text{for} \quad 50 \leqslant Pe \leqslant 1000 \tag{59}$$

$$L^*_{th,H} = 0.006977+0.1438/Pe, \quad \text{for} \quad 1 \leqslant Pe \leqslant 5 \tag{60}$$

$$L^*_{th,H} = 0.00854+0.1386/Pe, \quad \text{for} \quad 5 \leqslant Pe \leqslant 20 \tag{61}$$

$$L^*_{th,H} = 0.01106+0.08572/Pe, \quad \text{for} \quad 20 \leqslant Pe \leqslant 1000. \tag{62}$$

Again $N_H(\infty)$ values at $Pe = 1000$ for the case of constant heat flux are lower (6.8% and 6.7%) than the value of 0.0364 given in Shah and London [1]; however, the thermal entrance lengths of 0.01150 and 0.01151 are almost identical to their value (0.01154).

Table 10. Parallel plates: $N_H(\infty)$ and $L^*_{th,H}$ for the initial and boundary conditions of Fig. 3(a)

Pe	$N_H(\infty)$	$L^*_{th,H}$
1	2.6963	0.2907
2	1.2911	0.1355
5	0.4038	0.04979
10	0.1343	0.02713
20	0.07112	0.01736
50	0.04187	0.01281
100	0.03789	0.01190
200	0.03514	0.01161
1000	0.03392	0.01150

Table 11. Parallel plates: $N_H(\infty)$ and $L^*_{th,H}$ for the initial and boundary conditions of Fig. 3(b)

Pe	$N_H(\infty)$	$L^*_{th,H}$
1	0.2861	0.1511
2	0.1448	0.07794
5	0.07296	0.03631
10	0.04850	0.02229
20	0.03729	0.01555
50	0.03311	0.01232
100	0.03370	0.01173
200	0.03385	0.01156
1000	0.03395	0.01151

5. CONCLUSION

In the present study, numerical results have been obtained for laminar heat transfer in the entrance region of a circular duct and parallel plates. With the fully developed velocity field, both constant wall temperature and constant wall heat flux boundary conditions, with isothermal and adiabatic walls upstream from the entrance, have been investigated. The energy equations have been solved more accurately than previously with the use of the Richardson extrapolation to zero mesh size. Heat transfer results have been presented in terms of Nusselt number, incremental heat transfer number and thermal entrance length. Predicted fully developed Nusselt numbers compare very well with results in Shah and London. The correlations presented, which cover the entire Pe range and all the quantities considered, provide the much needed data for use in design of heat exchangers.

REFERENCES

1. R. K. Shah and A. L. London, *Laminar Flow Forced Convection in Ducts.* Academic Press, New York (1978).
2. T. V. Nguyen and I. L. Maclaine-cross, Incremental pressure drop number in parallel-plate heat exchangers, *J. Fluids Engng* **110**, 93–96 (1988).
3. T. V. Nguyen and I. L. Maclaine-cross, Simultaneously developing, laminar flow. Forced convection in the entrance region of parallel plates, *J. Heat Transfer* **113**, 837–842 (1991).
4. T. V. Nguyen, Low Reynolds number simultaneously developing flows in the entrance region of parallel plates, *Int. J. Heat Mass Transfer* **34**, 1219–1225 (1991).
5. I. L. Maclaine-cross, A theory of combined heat and mass transfer in regenerators, Ph.D. thesis, Department of Mechanical Engineering, Monash University, Australia (1974).
6. B. P. Leonard, A stable and accurate convective modelling procedure based on quadratic upstream interpolation, *Comp. Meth. Appl. Mech. Engng* **19**, 59–98 (1979).
7. T. V. Nguyen, I. L. Maclaine-cross and G. de Vahl Davis, The effect of free convection on entry flow between horizontal parallel plates. In *Numerical Methods in Heat Transfer* (Edited by R. W. Lewis, K. Morgan and O. C. Zienkiewicz), Chap. 16. Wiley, Chichester (1981).
8. D. K. Hennecke, Heat transfer by Hagen–Poisseuille flow in the thermal development region with axial conduction. *Wärme- und Stoffübertrag* **1**, 177–184 (1968).
9. C. J. Hsu, An exact analysis of low *Pe* number thermal entry region heat transfer in transversely nonuniform velocity fields, *A.I.Ch.E. Jl* **17**, 732–740 (1971).

TRANSFERT THERMIQUE LAMINAIRE POUR UN ECOULEMENT EN ETABLISSEMENT THERMIQUE DANS UN CONDUIT

Résumé—On présente le transfert thermique laminaire dans la région d'entrée d'un tube circulaire et de plaques parallèles. Le profil de vitesse est pleinement développé et la température est supposée uniforme en amont. L'équation de l'énergie aux différences finies qui tient compte de la conduction axiale est résolue par les méthodes ADI et QUICK et les résultats sont extrapolés à une taille de maille nulle avec l'extrapolation de Richardson. Le nombre de Nusselt local, le nombre incrémentiel de transfert et la longueur d'établissement thermique sont présentés pour *Pe* entre 1 et 1000, pour une température pariétale uniforme ou pour un flux thermique pariétal uniforme. Des formules pratiques précises pour l'effet du nombre de Peclet sur ces grandeurs sont proposées.

WÄRMEÜBERGANG BEI DER THERMISCH NICHT ENTWICKELTEN LAMINAREN STRÖMUNG IN KANÄLEN

Zusammenfassung—Es wird der Wärmeübergang bei laminarer Strömung im Einlaufgebiet in einem Kreisrohr und zwischen parallelen Platten beschrieben. Das Geschwindigkeitsprofil ist vollständig ausgebildet, und es wird angenommen, daß die Temperatur in unendlicher stromaufwärtiger Entfernung gleichförmig ist. Die Energiegleichung wird in Form finiter Differenzen formuliert, wobei axiale Wärmeleitung berücksichtigt wird. Die Lösung erfolgt mittels ADI und QUICK. Die Ergebnisse werden für die Maschengröße Null mit Hilfe der erweiterten Richardson-Extrapolation bestimmt. Die örtliche Nusselt-Zahl und die thermische Einlauflänge werden für Peclet-Zahlen zwischen 1 und 1000 und für konstante Wandtemperatur sowie konstante Wärmestromdichte an der Wand bestimmt. Schließlich wird eine genaue ingenieurmäßige Korrelation für den Einfluß der Peclet-Zahl auf diese Größen ermittelt.

ЛАМИНАРНЫЙ ТЕПЛОПЕРЕНОС ПРИ ТЕРМИЧЕСКИ РАЗВИВАЮЩЕМСЯ ТЕЧЕНИИ В КАНАЛАХ

Аннотация—Описывается ламинарный теплоперенос на входном участке канала круглого сечения и параллельных пластин. Предполагается, что на бесконечности профиль скорости является полностью развитым, а температура однородна. С использованием неявного метода переменных направлений и метода QUICK решается конечно-разностное уравнение, соответствующее уравнению энергии с учетом аксиальной теплопроводности, и для полученных результатов используется модифицированная экстраполяция Ричардсона. Приводятся локальные характеристики теплопереноса и длина входного теплового участка для значений *Pe*, изменяющихся в интервале 1–1000 в случае граничных условий с постоянной температурой стенки и постоянным тепловым потоком на ней. Получены точные соотношения, позволяющие оценить влияние числа Пекле на исследуемые вличины.